Image enhancement method based on multi algorithm fusion

Xinyu Gao*

Department of Computer Science and Engineering, North China Electric Power University, Baoding, Hebei, 071066

*Corresponding author: 18835258627@163.com

Abstract. This research suggests an image enhancement method based on multi algorithm fusion. The illumination component and reflection component are obtained by morphological closure. On the one hand, multiple inputs of the estimated illumination and the corresponding weights are fused by multi-scale fusion technology. On the other hand, space conversion technology is used. Two adjusted images are obtained based on multi-scale Gaussian filter and adaptive brightness enhancement algorithm. Then details are extracted from these two images through PCA fusion strategy. The reflection component is improved significantly after above operations. Finally, combine the illumination and reflection components. Compared with the classical algorithm, our method can simultaneously achieve brightness improvement, naturalness maintenance and contrast enhancement.

Keywords: fusion, multi-scale, adaptive image enhancement, PCA

1. Introduction

Nowadays, improving the image in low light has emerged as one of the hot topics in the world of machine vision research [1]. In this paper, we propose a fusion based method to enhance the low light images without multiple images of the same scene [2-4].

1.1. Related work

The current image enhancement algorithms mainly include: histogram-based method [5-14], Retinex-based method [15-19] and filtering-based method [20-26].

Traditional histogram-based methods include HE [6] and CLAHE [7]. Among them, HE algorithm can enrich image details by evenly extending the image histogram on the whole gray level. However, in the process of histogram balancing, it will lead to local image over enhancement and detail loss [12].

In the 1970s, Retinex theory was initially developed by an American physicist named Edwin Land [27]. With the emergence of Retinex theory, Retinex-based algorithms also appear. The first Retinex-based algorithm is a random path algorithm proposed by Land et al [28,29]. Based on Land's Mondrian global model, Retinex algorithm based on Poisson equation was also proposed successively [30,31]. McCann algorithm [32] is a Retinex algorithm based on multiple iteration strategy. Subsequently, Funt proposed the McCann99 algorithm and used the Gaussian pyramid model for layer by layer iteration [33]. At present, Retinex algorithm which is widely accepted by the public is based on the algorithm of center surround mode. Common algorithms of center surround mode include SSR algorithm and MSR algorithm [17]. In recent years, Retinex algorithm based on variable frame estimated brightness image by iterative solution of variable frame equation, then enhanced it by subtracting brightness image from original image, achieving good enhancement effect [13,19]. The image enhancement algorithm based on Retinex theory has obvious shortcomings. In places with strong contrast between light and shade, the halo phenomenon will directly affect the image quality. In addition, the large amount of computation is also a problem to be solved.

Filtering-based method is the last traditional method. One of the most representative algorithms is unsharp masking algorithm (GUM) [21]. In addition, automatic exposure correction on the image area [22], combination of illumination from natural light images and details from flash images [23] are also image filtering based methods.

1.2. Method Overview

Our proposed method has a relatively good enhancement effect for very weak illumination conditions. And the main idea of it is outlined below.

First, the method separates the light component from the reflection component. According to "the dark channel prior" [34], the brightness variance is obtained by calculating the greatest value among the three-color channels. And the illumination is calculated after morphological closure operation and guided filter function refinement. The reflection component is obtained based on Retinex theory [35]. This step can calculate and estimate the illumination and reflection component effectively in fewer computation steps, reducing the time complexity.

Secondly, in order to combine the advantages of different image enhancement algorithms, two new inputs are derived to improve the global brightness and local contrast respectively. Corresponding weights are designed for each input. They are exposure weight, color contrast weight and fusion weight. After that, the multi-scale pyramid technique is introduced to integrate the input and corresponding weights to obtain the adjusted illumination components.

Thirdly, in order to enhance the reflection component, space conversion technology is used and then extract the V component. In order to combine the advantages of filtering-based method, a multi-scale Gaussian filter is constructed to obtain coarse layer image and detail layer image. After that a simple linear combination method is used to integrate coarse layer image and detail layer image. And then two images are obtained by adjusting the parameter of the adaptive image enhancement function with the fused image as a correction factor. Finally, the image was fused by PCA algorithm, and the adjusted reflection component was obtained after space conversion.

Finally, the light and reflection components are fused.

Next, in the Section 2, the algorithm developed in this paper is fully described. In the Section 3, the performance of this method is tested from quantitative and qualitative perspectives. In the section 4, we will sum up the algorithm and draw conclusions.

2. Proposed fusion-based algorithm

The algorithm is divided into the following four steps, which correspond to the following four sections (1) Estimation of illumination component and reflection component, (2) Enhancement of illumination component, (3) Enhancement of reflection component, (4) fusion. Figure 1 depicts the algorithm process:

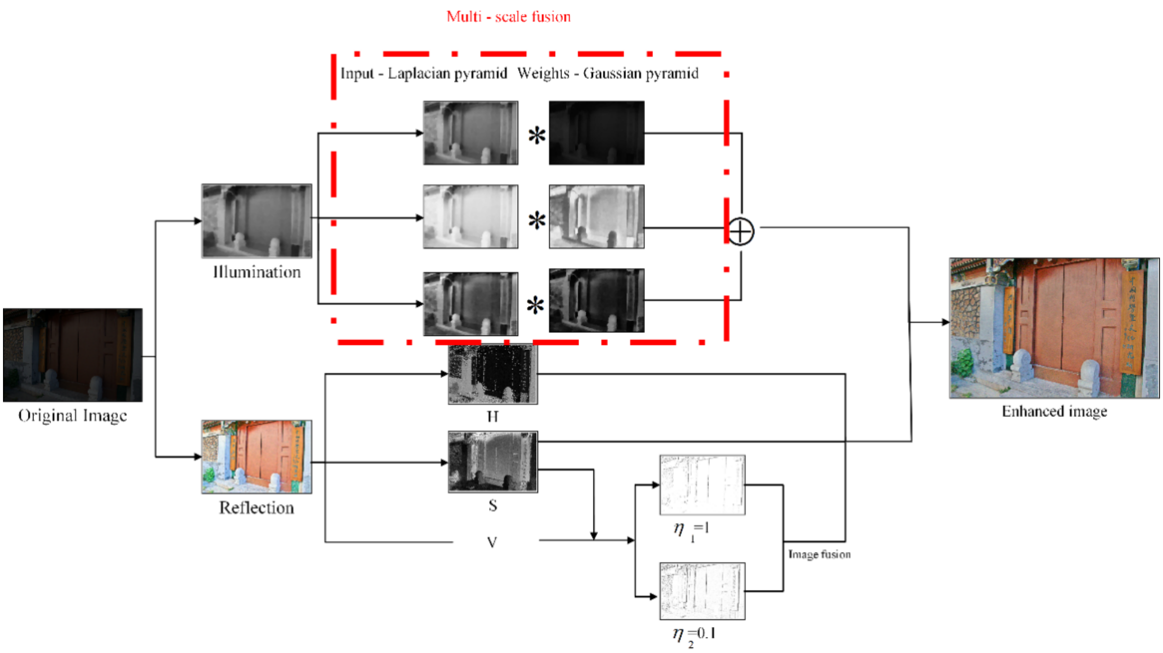

Figure 1. The algorithm enhances the image based on multi algorithm fusion.

2.1. Step 1: Estimation of illumination component and reflection component

The algorithm for illumination estimation is designed as follows. First, calculate the local minimum values of the three-color channels by analogy with the dark channel prior [37], The brightness variance I is obtained by the following formula:

$$I(x,y) = \max_{c\in[R,G,B]} P^c(x,y) \tag{1}$$

As the *illumination* image is locally smooth, it is necessary to use some operations to refine it. Morphological closing operation is selected to smooth the input finally — firstly the image dilation operation is performed and then the image etching operation. The morphological closure expression is as follows:

$$Q = \frac{I \bullet O}{255} \tag{2}$$

O represents morphological closing operation, $\bullet$ represents the closing operation. The formula converts the operation range to [0,1] by dividing by 255. After a large number of experiments and comparison, the disk structure element is used and the radius is specified as 7, so that the maximum gap in the image can be filled to get the best experimental results [36].

After smoothing, the estimated illumination image is further refined by guided filter function. The mathematical formula of the filter is as follows:

$$Q_i = \sum_j W_{ij}(v) Q_j \tag{3}$$

In the formula, i and j are the pixel index, and W is the filter kernel only related to the guide image v. The guided filter kernel function can be given by the following formula:

$$W_{ij}(v) = \frac{1}{|\omega|^2} \sum_{k:(i,j)\in\omega_k} \left(1 + \frac{(v_i - \varphi_k)(v_j - \varphi_k)}{\theta_k^{\,2} + \varepsilon} \right) \tag{4}$$

ω_k is the window whose center is pixel k, the window's pixel count is ω, the mean and variance of v are denoted by φ_k and θ_k^2. The guide image v obtained in this paper is the V layer.

Based on the Retinex theory [38], the reflection component can be obtained by using the following formula:

$$P(x,y) = I(x,y) R(x,y) \tag{5}$$

P is the input low- light image, R is the reflection component, and L is the illumination component.

2.2. step 2: Enhancement of illumination component

2.2.1. Input and corresponding weight calculation

At this time, the estimated illumination image quality is still very poor. On the one hand, the low-light areas lack the brightness improvement; On the other hand, the contrast degrades near the underexposed area. In this paper, three initial images are obtained by different processing of images.

The V channel of the initial estimated illumination image, which holds the fundamental makeup of the original image, serves as the initial input image.

The next input can effectively improve the global brightness:

$$Q_2(x,y) = \frac{2}{\pi} \arctan\left(\lambda Q(x,y)\right) \tag{6}$$

λ changes with the brightness of different images. After research, we set the value as:

$$\lambda = 10 + \frac{1 - Q_{mean}}{Q_{mean}} \tag{7}$$

Q_{mean} represents the estimated illumination Q's average value. It can be seen from the formula that λ and Q_{mean} are inversely proportional. The higher λ, the greater the enhancement.

The third input is calculated by CLAHE [7]. At the cost of reducing the overall brightness, the noise is suppressed effectively.

Next, to improve the suitability of the output for visual perception, the three initial images obtained in the above steps are fused, and the corresponding weights of each image are designed as follows.

The exposure weight represents the exposure level of the image. "Neither an overexposed nor an underexposed image should be acceptable." Based on the above conclusion, we design the following weight coefficient:

$$W_{L,k}(x,y) = \exp\left(-\frac{\left(Q^k(x,y)-\mu\right)^2}{2\sigma^2}\right) \tag{8}$$

K is the index of the inputs, μ is the mean value, σ is the standard deviation. The article assumes μ =0.5, σ =0.25.

The second weight is the color contrast weight, which is calculated according to the chroma filtering formula [37].

$$W_{C,k}(x,y) = Q_k(x,y)\left(1+\cos\left(\beta H(x,y)+\eta\right)S(x,y)\right) \tag{9}$$

The paper sets β =2 and $\eta = 250^{\circ}$, which has the highest contrast and the best experimental results.

the fusion weight is calculated and normalized according to the first and second weights:

$$W_k(x,y) = W_{L,k}(x,y)W_{C,k}(x,y) \tag{10}$$

$$\overline{W_k}(x,y) = \frac{W_k(x,y)}{\sum_k W_k(x,y)} \tag{11}$$

Figure 2 shows the three inputs and their respective weights. The area with the required high contrast is given a significant amount of weight in the paper.

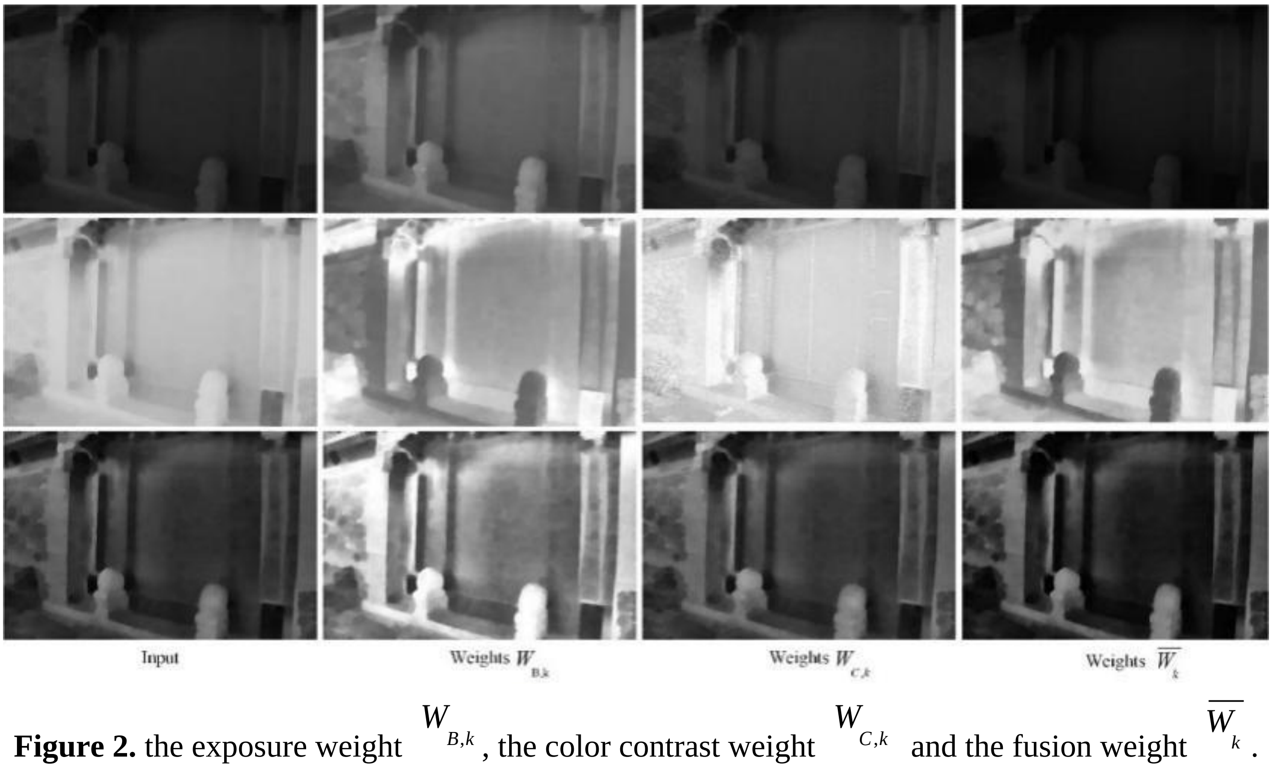

Figure 2. the exposure weight $W_{B,k}$, the color contrast weight $W_{C,k}$ and the fusion weight $\overline{W_k}$.

2.2.2. Multiscale fusion

This paper chooses to use multiscale pyramid technology [38] instead of simple fusion. Each source input is disserted into Laplace pyramid, and the normalized weight map is disserted into Gaussian pyramid. Assuming that Gaussian and Laplace pyramid have the same number of layers, the fusion weight is equal to:

$$F^c(x,y) = \sum_k G^c\left\{\overline{W^k}(x,y)\right\} L^c\left\{Q^k(x,y)\right\} \tag{12}$$

Where c represents the number of pyramid levels and 0<c<N. In practice, N depends on the size of the image. $L\{Q^k\}$ represents the Laplace pyramid formed by input decomposition and $G\{\overline{W}\}$ represents the weight mapping of Gaussian pyramid. Compared with the sharp change of weight map in simple fusion, this method mixes image features rather than image intensity. So it will not produce obvious seams [34] and can get a better fusion result of estimated illumination image.

$$I_{final}(x,y) = \sum_c U_d\left(F_c(x,y)\right) \tag{13}$$

U_d is the up-sampling operator, where $d = 2^{c-1}$.

2.3. step 3: Enhancement of reflection component

Inspired by the adaptive image enhancement algorithm, the paper adjusts the parameters adaptively of the enhancement function.

2.3.1. coefficient: Space conversion

Research shows that converting RGB images to HSV images for processing can effectively prevent color distortion. Here is the mathematical expression of space conversion:

$$\begin{cases} V = \max(R,G,B) \\ S = 1 - \dfrac{\min(R,G,B)}{V} \\ H = \begin{cases} 60 \times \dfrac{G-B}{V-\min(R,G,B)} & if\ V = R \\ 120 + \dfrac{60 \times (B-R)}{V-\min(R,G,B)} & if\ V = G \\ 240 + \dfrac{60 \times (R-G)}{V-\min(R,G,B)} & if\ V = B \end{cases} \end{cases} \tag{14}$$

Where, R, G and B are the red, blue and green channels in RGB color space; H, S and V represent hue, saturation and brightness space respectively.

2.3.2. V component enhancement

Here, we use the Gaussian function to compress the dynamic range of the original image and accurately extract the illumination component. To take into account the compression of dynamic range and color high fidelity at the same time, a group of multi-scale Gaussian filters are constructed in Gaussian scale space:

$$R_{v\_g}(x,y) = \sum_{i=1}^{N} \theta_i \left[R_v(x,y) * G_i(x,y) \right] \tag{15}$$

The scaling parameters are represented by the integer N, $R_v(x,y)$ is the input image, $R_{v\_g}(x,y)$ is the estimated illumination component, $G_i(x,y)$ represents the Gaussian function with the ith scaling parameter and θ_i stands for the weight of the Gaussian function with the ith scaling parameter. Through experiments, the high, medium and low scale parameters are selected as 250, 80 and 15 respectively. And the correlation weight of Gaussian function composed of each scale parameter is set as 1/3. Figure 3 displays the Gaussian components extracted by the three-scale Gaussian function.

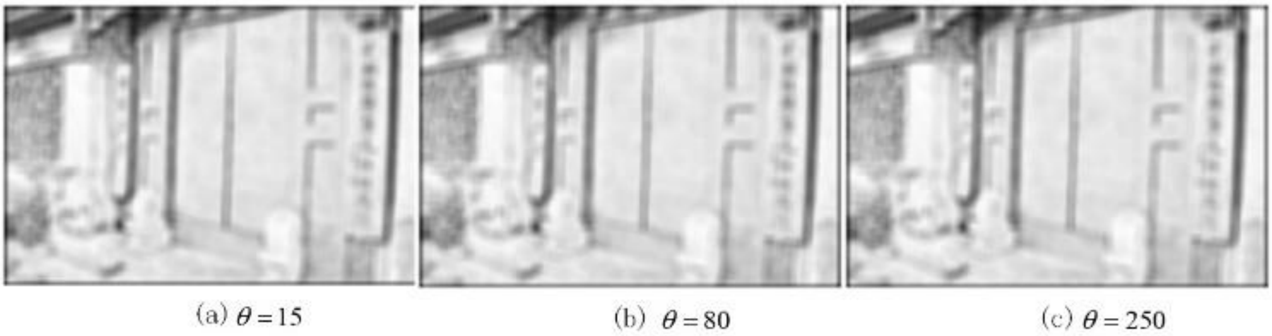

Figure 3. Extractions of the illumination component at different scales.

2.3.3. Adaptive brightness enhancement

An adaptive approach of illumination correction is proposed in this research. When the area has strong illumination and belongs to high brightness area, the adaptive brightness correction function plays a role in suppressing brightness; When the image brightness is low and the illumination component is lower than the brightness value of the region, the function plays the role of enhancing the brightness. The derivation process of adaptive brightness correction function is as follows:

It can be deduced from Weber-Fisher law that there is a logarithmic relationship between subjective brightness and objective brightness, namely:

$$R_v' = \beta \lg(R_v) + \beta_0 \tag{16}$$

Where β and β_0 are both constants.

To simplify the calculation, the following function is used to replace the above curve:

$$R_v' = \frac{R_v(255+k)}{R_v + k} \tag{17}$$

In the formula, k is the correction coefficient. The amount of image enhancement increases with decreasing value. To limit image enhancement, use the following formula:

$$R_v' = \frac{R_v(255+k)}{\max(R_v, R_{v\_g}) + k} \tag{18}$$

R_v is the V component, R_{v_g} is the estimated illumination component, R_v' is the enhanced image. Through experiments, the adjustment coefficient k is obtained from the following formula:

$$k = \eta \times S = \eta \times \frac{1}{W}\sum_{i}^{W} S_i \tag{19}$$

η is the weight coefficient, W is the total number of image pixels, S is the S component of the reflection component. After the operations above, the image contrast and brightness have been significantly improved. The paper let $\eta_1 = 0.1$ and $\eta_2 = 1$.

2.3.4. Image fusion technology based on PCA

The following formula is the weighted fusion algorithm:

$$F = \sum_{i=1}^{N} \omega_i S_i \tag{20}$$

F is the fused image, S_i is the original image, ω_i is the weight coefficient. PCA is used to determine the value of the weight coefficient.

PCA algorithm flow is as follows:

Assume that there are N original images in total, take each original image as an N-dimensional vector, and record it as X_k, $k = 1, 2, \ldots, N$.

(1) Construct data matrix from original image.

$$X = \left[x_1, x_2, \ldots, x_N \right] \tag{21}$$

(2) Determine the data matrix X's covariance matrix C.

$$C = \begin{bmatrix} \sigma_{11}^2 & \cdots & \sigma_{1j}^2 & \cdots & \sigma_{1N}^2 \\ \vdots & \ddots & \vdots & \ddots & \vdots \\ \sigma_{i1}^2 & \cdots & \sigma_{ij}^2 & \cdots & \sigma_{jN}^2 \\ \vdots & \ddots & \vdots & \ddots & \vdots \\ \sigma_{N1}^2 & \cdots & \sigma_{Nj}^2 & \cdots & \sigma_{NN}^2 \end{bmatrix} \tag{22}$$

Where σ_{ij}^2 is the variance of X.

$$\sigma_{ij}^2 = \frac{1}{n} \sum_{l=0}^{n} \left(x_{i,l} - \overline{x}_i \right) \left(x_{j,l} - \overline{x}_j \right) \tag{23}$$

Where, $\overline{x}_i$ is the typical value of the ith vector.

(3) Calculate the eigenvalues λ and the corresponding eigenvectors ξ of the covariance matrix C. Then, calculate the eigenvalue λ_i and the corresponding eigenvector ξ_i $(i = 1, 2, \cdots, m)$ according to the eigenvalue equation $|\lambda I - C| = 0$.

(4) Determine the weighting factor ω_i

$$\omega_i = \frac{\lambda_i}{\sum_{i=1}^{m} \lambda_i} \tag{24}$$

(5) Identify the fused output F

$$F = \sum_{i=1}^{m} \omega_i S_i \tag{25}$$

Here, N=2 and the η value of the images used for fusion is 0.1 and 1 respectively. The algorithm flow is shown in Figure 4 when N=2.

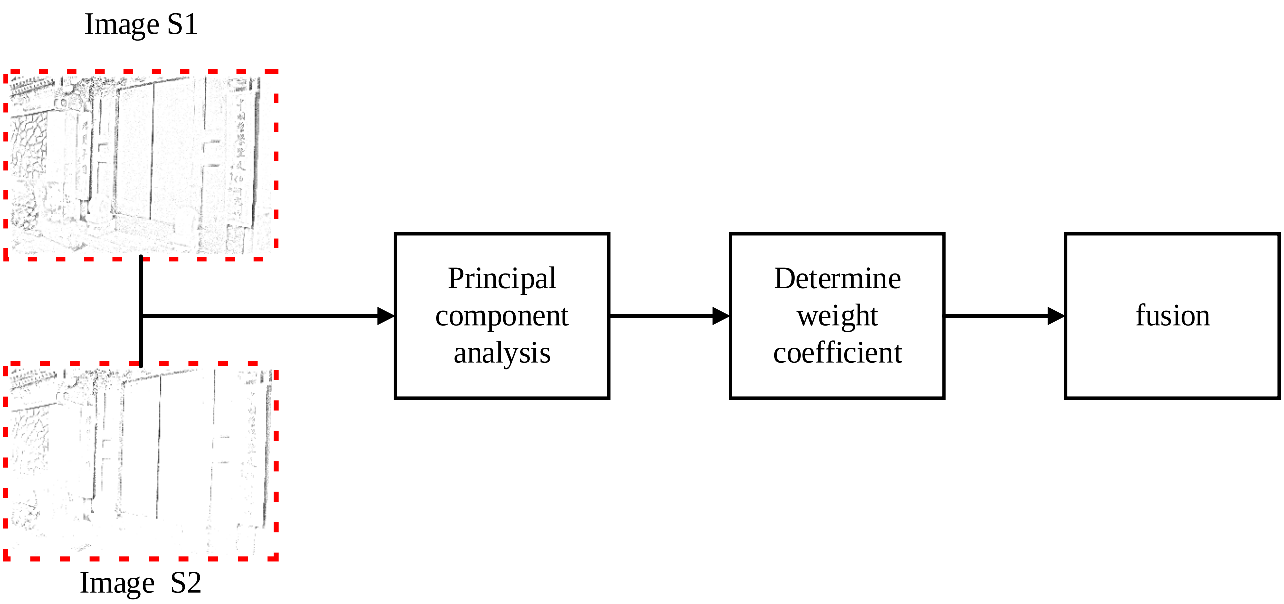

Figure 4. Image fusion based on principal component analysis

2.3.5. Space conversion

Convert HSV images to RGB images.

2.4. step 4: fusion

The function is as follows [35]:

$$S_{enhanced}(x,y) = I_{final}(x,y)F(x,y) \tag{26}$$

Where, $I_{final}(x,y)$ and $F(x,y)$ are the adjusted illumination and reflection components.

3. Experimental results and discussion

In this section, we highlight the experimental results to demonstrate the proposed fusion method's superior performance over existing approaches. In order to prove that our algorithm is effective, we construct an experimental laptop-based platform (Intel corei7-10750H CPU). Matlab2020a is the testing software.

3.1. Subjective visual evaluation

So as to compare the methods effectiveness, we examine an extensive amount of images in low light and compare the proposed method with the other five methods. The five methods are: two Retinex-based method SRLIE [16] and RBMA [15], a histogram-based method, CVC [11], and a filtering-based method GUM [21].

We show four groups of images in figure 5 and each group of images includes the initial image and five enhanced images. In addition, to make readers better distinguish the improvement effect of each algorithm, this paper will enlarge and display the representative image area below each group of images. In the results of the 'Swimming pool' image in Figure 5, the images enhanced by CVC are all unnatural and gray, and GUM does not achieve significant enhancement. In the results of the 'Lighthouse' image and the 'woman' image, CVC and GUM can not enhance brightness very well, but the contrast has been improved. In the results of the 'Green Plant', the image enhanced by CVC shows serious color deviation. Although the images enhanced by GUM keep natural, there are still some dark areas which cannot be improved. After observation, we find that RBMA, SRLIE and the proposed method effectively improves all of the images. But the image edges have a jagged shape enhanced by RBMA. The brightness improvement of SRLIE enhanced images is not as obvious as the proposed method. And SRLIE has a fatal problem of can not being able to enhance the large input images.

In general, our method can enhance weak illumination images and uneven illumination images better than other methods. It can simultaneously achieve brightness improvement, naturalness maintenance and contrast enhancement.

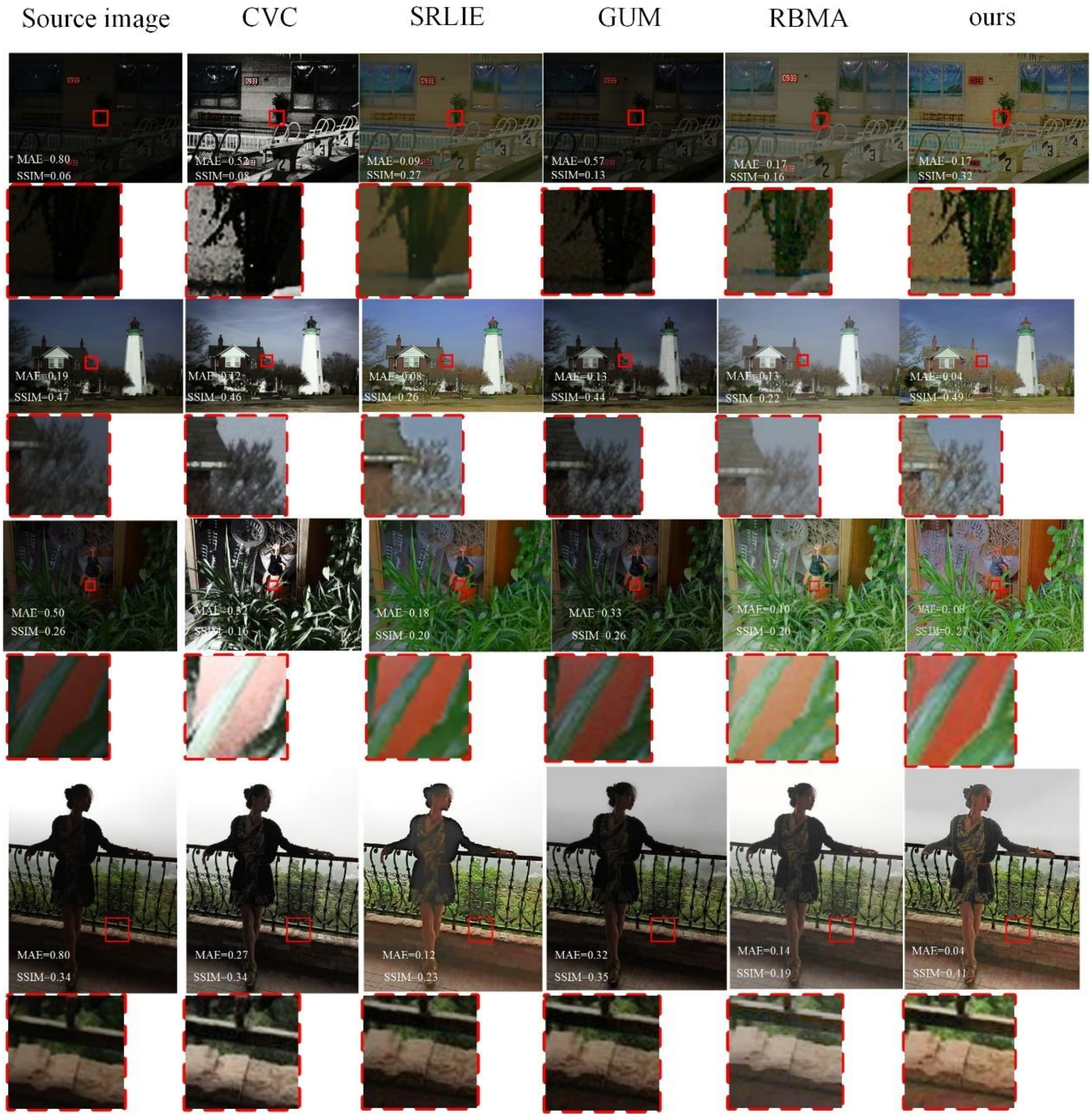

Figure 5. Visual comparison of images, from the top to bottom, shows the results of ‘Swimming pool’ image, ‘Lighthouse’ image, ‘Green plant’ image and ‘Woman’.

3.2. Objective visual evaluation

In addition to qualitative analysis, so as to ensure the research is rigorous, the image quality through algorithms should be evaluated. Here, we select two full reference IQA indicators to evaluate the enhanced images, namely SSIM and MAE. The formulas of SSIM and MAE are listed below:

$$SSIM(x,y)=\frac{(2\eta_x\eta_y+c_1)(2\delta_{xy}+c_2)}{(\eta_x^{\,2}+\eta_y^{\,2}+c_1)(\delta_x^{\,2}+\delta_y^{\,2}+c_2)} \tag{27}$$

Where, η_x and η_y are the mean value of image brightness, δ_x and δ_y are the standard deviation, δ_{xy} is the covariance, c_1 and c_2 always take a small normal number. Image quality is positively correlated with SSIM index values.

$$MAE = \frac{1}{m}\sum_{i=0}^{m}\left|y_i - y_i'\right| \tag{28}$$

Where, y_i is the actual value and y_i' is the predicted value. Image quality is inversely correlated with MAE index value.

Table.1 shows the MAE and SSIM values of each image enhancement method. It can be seen that the images quality enhanced by the proposed method is the best.

Table 1. The averages of MAE(M) and SSIM(S)

Image	Original		CVC		SRLIE		GUM		RBMA		Proposed	
	M	S	M	S	M	S	M	S	M	S	M	S
Average	0.47	0.28	0.31	0.26	0.12	0.24	0.34	0.29	0.14	0.19	**0.08**	**0.37**

4. Conclusion

This paper proposes a universal fusion framework, which can fuse various mature enhancement methods mentioned in this paper, and maximize the image enhancement effect by combining the advantages of each fusion algorithm. First, the initial input is decomposed into illumination component and reflection component. Secondly, the paper applies multi-scale fusion strategy to enhance the illumination component. Finally, the study constructs the adaptive enhancement function and enhance reflection component through PCA algorithm. Through quantitative and qualitative experiments, this method shows better performance than image enhancement algorithms such as MSR and GUM.

References

[1] T. Wang, Z. Ji, and Q. Sun, et al, “Label propagation and higher-order constraint-based segmentation of fluid-associated regions in retinal SD-OCT images,” Inform. Sci. 358, pp. 92–111, 2016.

[2] Z. Zhou, S. Li, and B. Wang, “Multi-scale weighted gradient-based fusion for multi focus images,” Inf. Fusion 20, pp. 60–72, 2014.

[3] T. Mertens, J. Kautz, and F.V. Reeth, “Exposure fusion, in: Proceedings of 15th Pacifific Conference on Computer Graphics and Applications,” pp. 382–390, 2007.

[4] Z. G. Li, J. H. Zheng, and S. Rahardja, “Detail-enhanced exposure fusion,” IEEE Trans. Image Process, vol. 21, no. 11, pp. 4672–4676, 2012.

[5] C. Lee, C. Lee, and C. S. Kim, “Contrast enhancement based on layered difference representation of 2d histograms,” IEEE Trans. Image Process, vol. 22, no. 12, pp. 5372–5384, 2013.

[6] R. C. Gonzalez and R. E. Woods, “Digital Image Processing,” Prentice-Hall, Englewood Cliffs, NJ, USA, 2007.

[7] E. D. Pisano, S. Zong, B. M. Hemminger, “Contrast limited adaptive histogram image processing to improve the detection of simulated spiculations in dense mammograms, ” J. Digit. Imaging, vol. 11, no. 4, pp. 193-200, 1998.

[8] Y.T. Kim, “Contrast enhancement using brightness preserving bi-histogram equalization,” IEEE Trans. Consum. Electron, vol. 43, no. 1, pp. 1–8, 1997.

[9] D. Coltuc, P. Bolon, J. M. Chassery, “Exact histogram specifification,” IEEE Trans. Image Process, vol. 15, no. 5, pp. 1143–1152, 2006.

[10] T. Arici, S. Dikbas, and Y. Altunbasak, “A histogram modifification framework and its application for image contrast enhancement,” IEEE Trans. Image Process, vol. 18, no. 9, pp. 1921–1935, 2009.

[11] T. Celik and Tjahjadi, “Contextual and variational contrast enhancement,” IEEE Trans. Image Process, vol. 20, no. 12, pp. 3431–3441, 2011.

[12] H. Xu, G. Zhai, X. Wu, and X. Yang, "Generalized equalization model for image enhancement," IEEE Trans. Multimed, vol. 16, no. 1, pp. 68–82, 2014.

[13] C. Lee, C. Lee, and Y.Y. Lee, "Power-constrained contrast enhancement for emissive displays based on histogram equalization," IEEE Trans. Image Process, vol.21, no.1, pp. 80–93, 2012.

[14] T. Celik, "Spatial entropy-based global and local image contrast enhancement," IEEE Trans. Image Process, vol.23, no. 12, pp. 5298–5308, 2014.

[15] Al-Hashim, Mohammad Abid, Al-Ameen, and Zohair, "Retinex-Based Multiphase Algorithm for Low-Light Image Enhancement," Traitement du Signal: signal image parole, vol. 37, no. 5, pp. 733-743, 2022

[16] M. D. Li, J. Y. Liu, W. H. Yang, X. Y. Sun, and Z. M. Guo, "Structure-Revealing Low-Light Image Enhancement Via Robust Retinex Model," IEEE transactions on image processing : a publication of the IEEE Signal Processing Society, vol. 27, no. 6, 2018.

[17] D. J. Jobson, Z. U. Rahman, and G. A. Woodell, "A multi-scale Retinex for bridging the gap between color images and the human observation of scenes," IEEE Trans. Image Process, vol. 6, no. 7, pp. 965–976, 1997.

[18] R. Kimmel, M. Elad, and D. Shaked, "A variational framework for Retinex," Int. J. Comput. Vis, vol. 52, no. 1, pp. 7–23, 2003.

[19] M. K. Ng and W. Wang, "A total variation model for Retinex," SIAM J. Imaging Sci, vol. 4, no. 1, pp. 345–365, 2003.

[20] Q. Shan, J. Jia, and M. S. Brown, "Globally optimized linear windowed tone mapping," IEEE Trans. Vis. Comput. Graph, vol. 16, no. 4, pp. 663–675, 2010.

[21] G. Deng, "A generalized unsharp masking algorithm," IEEE Trans. Image Process, vol. 20, no.5, pp.1249–1261, 2011.

[22] L. Yuan, J. Sun, "Automatic exposure correction of consumer photographs, in: Proceedings of European Conference on Computer Vision," pp. 771–785, 2012.

[23] E. Eisemann, F. Durand, "Flash photography enhancement via intrinsic relighting," ACM Trans. Graph (Proc. SIGGRAPH), vol. 23, no.3, pp. 673–678, 2004.

[24] E.P. Bennett and L. McMillan, "Video enhancement using per-pixel virtual exposures," ACM Trans. Graph (Proc. SIGGRAPH), vol. 24, no. 3, pp. 845–852, 2005.

[25] R. Fattal, D. Lischinski, and M. Werman, "Gradient domain high dynamic range compression," ACM Trans. Graph (Proc. SIGGRAPH), vol. 21, no. 3, pp. 249–256, 2002.

[26] Y. Wang, S. Zhuo, D. Tao, J. Bu, and N. Li, "Automatic local exposure correction using bright channel prior for under-exposed images," Signal Process, vol. 93, no. 11, pp. 3227–3238, 2013.

[27] E.H. Land and J.J. McCann, "Lightness and Retinex theory," J. Opt. Soc. Am, vol. 61, no. 1, pp. 1–11, 1971.

[28] E. Land, "The Retinex," Aiiler. Scient. Jun, vo1, 52, no. 2, pp. 247-264, 1964.

[29] E. Land and J. McCann, "Lightness and Retinex theory," J. Opt. Soc. Artier. Jan, vol. 61, no. 1, pp.1-11, 1971.

[30] R. Kimmel， M. Elad， D. Shaked， and R. Keshet, "Sobel. A variational framework for Retinex," Int. J. Comput. Vis, vol. 52, no. 1, pp.7-23, 2003.

[31] A. Hurlbert, "Formal connections between lightness algorithm," J. Opt. Soc. Amer, vol. 3, pp. 1 684-1 692, 1986.

[32] J. Frankle and J. McCann, "Method and apparatus for lightness imaging," US Patent, no. 4, 1983.

[33] B. Funt, F. Ciurea, and J. McCann, "Retinex in matlab," J. Electron. Imag. Jan, vol. 13, no. 1, pp. 48-57, 2004.

[34] K. He, J. Sun, and X. Tang, "Single image haze removel using dark channel prior," IEEE Trans. Pattern Anal. Mach. Intell, vol. 33, no. 12, pp. 2341 - 2353, 2011.

[35] E. H. L and J. J. McCann, "Lightness and Retinex theory," J. Opt. Soc. Am, vol. 61, no. 1, pp. 1-11, 1971.